



Article

Land Use Transitions and the Associated Impacts on Carbon Storage in the Poyang Lake Basin, China

Yiming Wang¹, Zengxin Zhang^{1,2,*}  and Xi Chen^{1,3} 

¹ State Key Laboratory of Hydrology-Water Resources and Hydraulics Engineering, College of Hydrology and Water Resources, Hohai University, Nanjing 210098, China; ymwang@hhu.edu.cn (Y.W.); xichen@hhu.edu.cn (X.C.)

² Joint Innovation Center for Modern Forestry Studies, College of Forestry, Nanjing Forestry University, Nanjing 210037, China

³ Institute of Surface-Earth System Science, School of Earth System Science, Tianjin University, Tianjin 300072, China

* Correspondence: zzhang@hhu.edu.cn

Abstract: Carbon storage plays an important role in the global carbon cycle and climate change mitigation. Understanding the relationship between land use change and carbon storage can significantly contribute to carbon neutrality and sustainable development. However, most previous studies only analyze the carbon storage change due to land use change, while few studies quantitatively evaluate the contributions of various land use transitions (LUTs) to carbon storage change, which cannot provide enough information for land use management. In the context of rapid urbanization and ecological conservation, the Poyang Lake basin (PYLB) has experienced dramatic land use change, which has significantly affected local carbon storage. Therefore, this study used the InVEST model to evaluate carbon storage in the PYLB from 1990 to 2020. Then, the Geo-information Tupu method was used to quantify the contributions of various LUTs to carbon storage change and identify the key LUTs. The results showed that carbon storage in PYLB decreased by 17.26 Tg from 1990 to 2020. The carbon gain was mainly attributed to transitions from ‘farmland to forestland’ (36.87%), ‘grassland to forestland’ (22.58%), and ‘farmland to water’ (15.89%). In contrast, the transitions from ‘farmland to built-up land’, ‘forestland to built-up land’, and ‘forestland to grassland’ contributed 39.94%, 28.06%, and 13.25% to carbon loss, respectively. Massive carbon loss caused by built-up land expansion should attract attention. This study can provide references for the formulation and optimization of land use policies to achieve carbon neutrality and sustainable development in the PYLB.

Keywords: carbon storage; InVEST model; Geo-information Tupu; land use transition; Poyang Lake basin



Citation: Wang, Y.; Zhang, Z.; Chen, X. Land Use Transitions and the Associated Impacts on Carbon Storage in the Poyang Lake Basin, China. *Remote Sens.* **2023**, *15*, 2703. <https://doi.org/10.3390/rs15112703>

Academic Editors: Sheng Wang, Suxia Liu, Yongqiang Zhou and Raphaél Payet-Burin

Received: 3 April 2023

Revised: 17 May 2023

Accepted: 22 May 2023

Published: 23 May 2023



Copyright: © 2023 by the authors. Licensee MDPI, Basel, Switzerland. This article is an open access article distributed under the terms and conditions of the Creative Commons Attribution (CC BY) license (<https://creativecommons.org/licenses/by/4.0/>).

1. Introduction

Global warming is becoming increasingly serious, which has threatened sustainable development and attracted worldwide attention [1,2]. Massive carbon emissions and human-induced land use change are considered two dominant driving forces of climate warming [3,4]. Carbon storage, as an important indicator of ecosystem function, is vital to the global carbon cycle and climate regulation [5,6]. Increasing carbon storage can effectively reduce the amount of CO₂ in the atmosphere, which is one of the most important ways to mitigate climate warming [7]. Since China has proposed the goal of carbon neutrality, methods to reduce carbon emissions and increase carbon storage in the ecosystem have become essential issues [8–10]. Effective evaluation of carbon storage is of great significance for climate change adaptation and sustainable development [11]. Moreover, it can also provide useful references for formulation and optimization of land use policies [12,13].

At present, the methods used to evaluate carbon storage mainly include field surveys, remote sensing, and model simulations. Although the results of field surveys are precise,

they are also time-consuming and laborious, which makes them more suitable for small scales [14,15]. The remote sensing method is very suitable for large scales because of its low cost and extensive coverage, while the accuracy of evaluation is influenced by the spatiotemporal dimensions of remote sensing data [16]. Model simulations have grown in popularity in recent years because they can spatially explicitly evaluate carbon storage at various scales [17,18]. Many models can be used to evaluate carbon storage, such as High Accuracy Surface Modeling (HASM) model [19], Century model [20], and Biome–Biogeochemical Cycles (Biome–BGC) model [21]. However, most of these models need a large amount of data and parameterization, which limits their application [11,22]. In contrast, the Integrated Valuation of Ecosystem Services and Tradeoffs Tool (InVEST) model has become increasingly popular in evaluating carbon storage due to its low input requirements and excellent output precision [5,18]. This model only needs remote sensing data (land use) and carbon density as inputs, and comprehensively considers four carbon pools: aboveground carbon, belowground carbon, dead organic carbon, and soil organic carbon. Since this model can link land use change and carbon storage, it has been widely used to quantify the effect of land use policies and ecological restoration programs on regional carbon storage [13,23–28].

Land use change is considered the dominant factor affecting carbon storage in terrestrial ecosystems [29]. In recent decades, China has experienced rapid urbanization, characterized by dramatic land use transitions (LUTs) from ecological land to built-up land, which has led to serious ecosystem degradation, including considerable loss of carbon storage [9,13]. Meanwhile, to mitigate ecosystem degradation, the Chinese government has also launched multiple ecological restoration programs, such as the Grain for Green program and natural forest conservation program, since the late 1990s [30]. Previous research revealed that these programs significantly increased ecosystem carbon storage [18,23,25,31,32]. However, most previous studies only analyzed the carbon storage change due to land use change, while few studies quantified the contributions of various LUTs to carbon storage change. Accurate quantification of contributions of various LUTs to carbon storage change can help identify the key LUTs affecting carbon storage and provide more detailed references for land use policies. Geo-information Tupu is a geographical spatiotemporal analysis method to explore the internal structure of geographic elements and the rules of spatial differentiation [33]. This method can record the composite spatiotemporal information of land use change based on Tupu units, which makes LUT research more accurate, intuitive, and realistic [34,35]. This method has been applied in many fields such as ecosystem service value [35], landscape multifunctionality [36], habitat quality [37], and landscape ecological risk [38].

The Poyang Lake basin (PYLB) plays an important role in ecological security in the middle-lower reaches of the Yangtze River [39]. In the context of rapid urbanization and ecological conservation, this basin has experienced dramatic land use change, which significantly affected local carbon storage. However, how carbon storage changed in the basin remains unclear. Therefore, this study utilized the InVEST model and Geo-information Tupu method to explore the effect of LUTs on carbon storage. The main objectives were to (1) assess the spatiotemporal change in land use and carbon storage in PYLB from 1990 to 2020; (2) quantify the contributions of various LUTs to carbon storage change and identify the key LUTs. This study can provide references for carbon neutrality and sustainable development in the PYLB.

2. Methods and Materials

2.1. Study Area

The PYLB (24°24'N–29°46'N, 113°23'E–118°46'E) covers an area of 1.62×10^5 km² (Figure 1). It consists of the Poyang Lake region and five subbasins (i.e., Ganjiang river basin, Fuhe river basin, Raohe river basin, Xinjiang river basin, and Xiushui river basin). This basin is dominated by a subtropical monsoon climate, with an annual temperature of approximately 17.6 °C and an annual precipitation of approximately 1680 mm [40]. The

topography of this basin is complex and diverse, with mountains, hills, and plains covering 36%, 42%, and 12.1% of the basin, respectively [41].

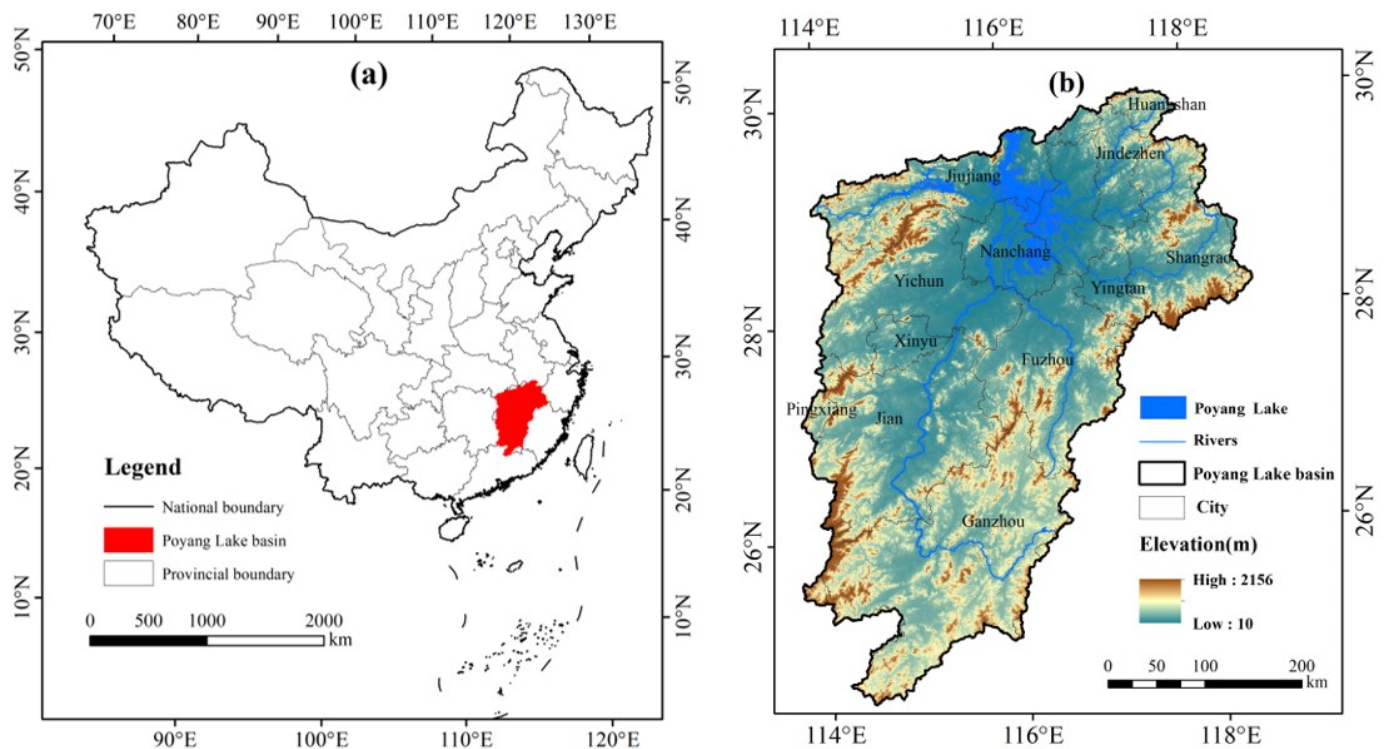


Figure 1. Location (a) and elevation (b) of the PYLB.

2.2. Methods

Figure 2 illustrates the research framework of this study. First, we used the Geo-information Tupu method to analyze land use transitions in the PYLB from 1990 to 2020. Then, the InVEST model was used to estimate carbon storage, due to its low input requirements and excellent output precision, and hotspot analysis was used to explore the spatiotemporal change in carbon storage. Finally, based on the results of the previous two steps, we quantified the contributions of different land use transitions to carbon storage change during each period and identified the key land use transitions, which can provide references for land use management in the PYLB.

2.2.1. Geo-Information Tupu Method

The Geo-information Tupu method can reflect the spatiotemporal change in land use using the Tupu unit [33]. The land use types of farmland, forestland, grassland, water area, built-up land, and unused land were assigned codes 1, 2, 3, 4, 5, and 6, respectively. Then, the Raster Calculator tool in ArcGIS 10.2 was used to build the Tupu process for LUT. The equation is as follows [35]:

$$T = A \times 10 + B \quad (1)$$

where T is the code of LUT during the study period, and A and B are the codes of land use type at the beginning and end of the study period, respectively.

2.2.2. The InVEST Model

The Carbon Storage and Sequestration module of InVEST model was utilized to assess carbon storage. This model has been widely used in carbon storage assessment, due to its low input requirements and excellent output precision [8,10–12,14,29]. It only needs land use data and carbon density as inputs, and comprehensively considers four carbon pools:

aboveground carbon, belowground carbon, dead organic carbon, and soil organic carbon. The equations are as follows:

$$C_{i_total} = C_{i_above} + C_{i_below} + C_{i_dead} + C_{i_soil} \quad (2)$$

$$CS = \sum_1^n C_{i_total} \times A_i, \quad (i = 1, 2, \dots, n) \quad (3)$$

where CS is the total carbon storage; C_{i_total} , C_{i_above} , C_{i_below} , C_{i_dead} , and C_{i_soil} are total carbon density and the carbon densities of aboveground carbon, belowground carbon, dead organic carbon, and soil organic carbon in land use type i , respectively; and A_i is the area of land use type i .

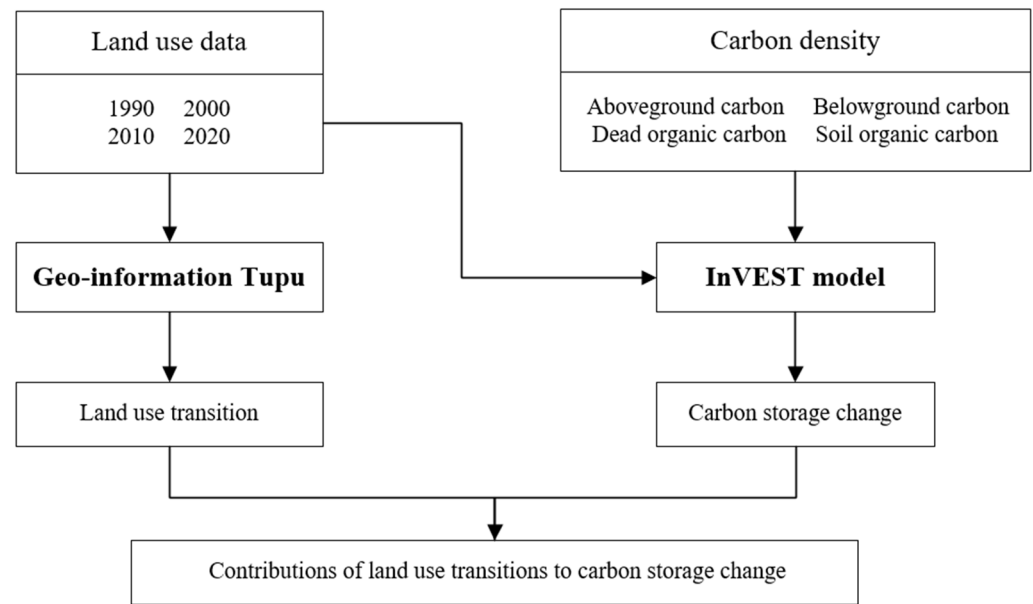


Figure 2. The research framework of this study.

2.2.3. Hotspot Analysis

The Getis–Ord G_i^* statistic can assess spatial high-value clusters and low-value clusters of regional elements and spatial patterns of hotspots, which can provide a scientific reference for land use policy [42]. This study applied the Getis–Ord G_i^* statistic to analyze the spatial agglomeration of carbon storage change. To enhance the visualization, we defined the sample unit as a $6 \text{ km} \times 6 \text{ km}$ grid, to cover the study area. The carbon storage changes in each grid were calculated. Then the hotspot analysis was conducted in ArcGIS 10.2. The equations are as follows [42]:

$$G_i^*(d) = \frac{\sum_{j=1}^n w_{ij} x_j - \bar{X} \sum_{j=1}^n w_{ij}}{S \sqrt{\frac{[n \sum_{j=1}^n w_{ij}^2 - (\sum_{j=1}^n w_{ij})^2]}{n-1}}} \quad (4)$$

$$\bar{X} = \frac{\sum_{j=1}^n x_j}{n} \quad (5)$$

$$S = \sqrt{\frac{\sum_{j=1}^n x_j^2}{n} - (\bar{X})^2} \quad (6)$$

where $G_i^*(d)$ is the z-score; n is the number of regions, and each region is identified with a point $i = 1, 2, \dots, n$, in which each point is connected with a value x (weight) from a variable X , where x_j denotes x associated with j points within distance d of the i th point; w_{ij} is a spatial weight matrix between i and j ; and \bar{X} and S are the sample mean and standard

deviation, respectively. If statistically significant, a higher z-score (z-score > 0) means that the hotspots (high values) are clustered more closely. A lower z-score (z-score < 0) means that the cold spots (low values) are tightly clustered. Non-significant spots are not statistically significant.

2.3. Data Sources

2.3.1. Land Use Data

The land use data from 1990, 2000, 2010, and 2020, with a spatial resolution of 30 m, were obtained from the Resource and Environment Science Data Center of the Chinese Academy of Sciences (<https://www.resdc.cn/>, accessed on 21 May 2022). Data production was based on Landsat Thematic Mapper/Enhanced Thematic Mapper (TM/ETM) remote sensing images from various periods that were generated through visual interpretation based on national field surveys. The accuracy of this dataset is greater than 92.90% [43]. In this study, the land use dataset was divided into six types: farmland, forestland, grassland, wetland, built-up land, and unused land.

2.3.2. Carbon Density Data

The total carbon density of each land use type contains four parts: carbon density in aboveground carbon, belowground carbon, dead organic carbon, and soil organic carbon. In this study, we first collected carbon density data in the study area from published papers that used scientific methods (e.g., field surveys and geochemical experiments). The carbon densities of farmland, forestland, and grassland were 106.30 Mg/ha, 124.30 Mg/ha, and 102.50 Mg/ha, respectively [44,45]. The carbon density of wetland was 140.68 Mg/ha [46]. The carbon densities of soil organic carbon of built-up land and unused land were 34.33 Mg/h and 34.42 Mg/ha, respectively [29,47]. Then, according to the proportion of the four carbon pools as to each measurement of carbon density for individual land use type in the literature [48], we calculated the four measurements of carbon density of four carbon pools for each land use type (Table 1).

Table 1. Carbon densities of each land use type in the PYLB.

	Carbon Density (Mg/ha)					References
	Aboveground Carbon	Belowground Carbon	Dead Organic Carbon	Soil Organic Carbon	Total	
Farmland	16.65	10.98	2.13	76.54	106.30	[29,44,45]
Forest	26.93	5.39	2.48	89.50	124.30	[29,44,45]
Grassland	12.11	14.54	2.05	73.80	102.50	[29,44,45]
Wetland	10.83	19.18	3.98	106.70	140.68	[29,45,46]
Built-up land	7.61	1.52	0.00	34.33	43.46	[29,45,47]
Unused land	10.36	2.07	0.96	34.42	47.81	[29,45,47]

3. Results

3.1. Land Use Change from 1990 to 2020

Forestland and farmland were the dominant land use types in the basin (Table 2 and Figure 3), accounting for 61.80% and 26.21% of the basin in 2020, respectively. Forestland was widely distributed in the basin and farmland was mainly concentrated in plain regions. Grassland, wetland, built-up land, and unused land occupied 4.45%, 4.46%, 3.08%, and 0.01% of the basin in 2020, respectively. The built-up land showed an accelerated upward trend, expanding by 15,989 ha, 102,031 ha, and 134,590 ha during 1990–2000, 2000–2010, and 2010–2020, respectively. The forestland increased by 22,665 ha during 1990–2000, while decreasing by 12,821 ha and 97,108 ha during 2000–2010 and 2010–2020, respectively. The farmland experienced an accelerating decreasing trend, decreasing by 19,215 ha, 35,381 ha, and 74,192 ha during 1990–2000, 2000–2010, and 2010–2020, respectively. The grassland decreased by 23,090 ha and 45,809 ha during 1990–2000 and 2000–2010, respectively, while

increasing by 32,073 ha during 2010–2020. The wetland decreased by 7738 ha during 2000–2010, while increasing by 3653 ha and 4750 ha during 1990–2000 and 2010–2020, respectively. The unused land exhibited a continual downward trend.

Table 2. Land use area and proportion in the PYLB from 1990 to 2020.

Land Use	1990		2000		2010		2020	
	Area (ha)	Percent (%)						
Farmland	4,379,812	27.01	4,360,597	26.89	4,325,216	26.67	4,251,024	26.21
Forestland	10,109,322	62.34	10,131,987	62.48	10,119,166	62.40	10,022,057	61.80
Grassland	757,781	4.67	734,691	4.53	688,883	4.25	720,956	4.45
Wetland	722,019	4.45	725,672	4.47	717,934	4.43	722,639	4.46
Built-up land	246,129	1.52	262,118	1.62	364,150	2.25	498,739	3.08
Unused land	2141	0.01	2139	0.01	1856	0.01	1788	0.01

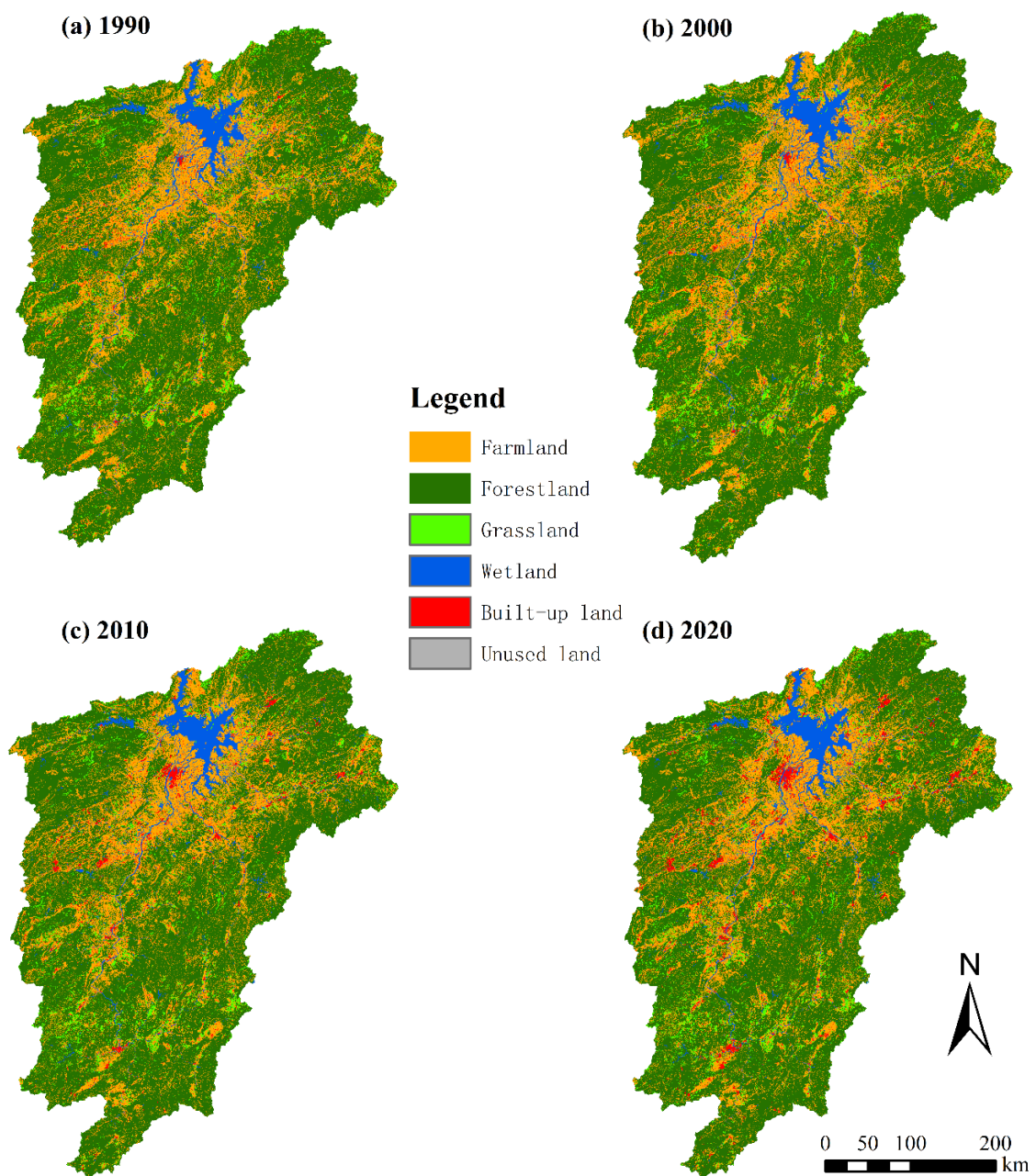


Figure 3. Spatial pattern of land use types of the PYLB.

3.2. Land Use Transitions from 1990 to 2020

Based on the Geo-information Tupu method, the land use transitions during the three periods (1990–2000, 2000–2010, and 2010–2020) were analyzed (Figure 4 and Table 3). The land use conversion areas were 122,424 ha, 374,721 ha, and 684,779 ha during 1990–2000, 2000–2010, and 2010–2020, respectively. From 1990 to 2000, forestland expansion was obvious, and “grassland to forestland” and “farmland to forestland” accounted for 28.72% and 14.06% of the changed land. Meanwhile, there were 12,257 ha and 12,182 ha of forestland converted to grassland and farmland, accounting for 10.01% and 9.95% of the total changed area. The built-up land expanded mainly by encroaching on farmland and forestland. There was 12,568 ha of farmland converted into wetlands during this period. During 2000–2010, farmland was mainly converted to built-up land and forestland, which accounted for 18.70%, and 14.15% of the changed area. Forestland was mainly converted to farmland and built-up land. Grassland was mainly converted to forestland, and wetland was mainly converted to farmland, which occupied 11.67% and 8.09% of the changed area. During 2010–2020, the transition from forestland to farmland occupied 24.28% of the changed area. Meanwhile, 163,130 ha of farmland was converted to forestland, accounting for 23.82% of the changed area. This was much higher than in the previous two periods. The built-up land mainly occupied farmland (93,059 ha) and forestland (56,380 ha). It is noteworthy that the area of “forestland to grassland” was much higher than that of “grassland to forestland” (62,716 ha vs. 23,469 ha). Conversion of “wetland to farmland” only accounted for 1.95% of the changed area, which was much lower than that during the previous two periods.

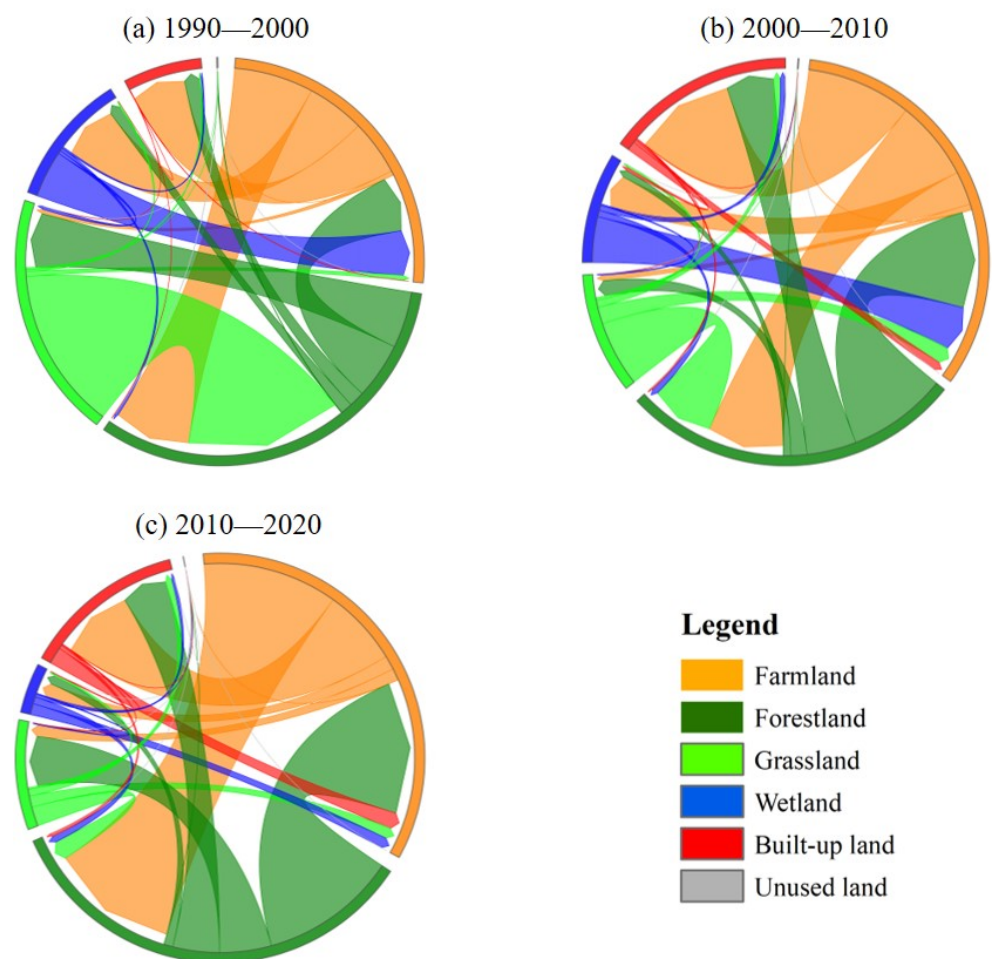


Figure 4. Land use transitions in the PYLB.

Table 3. Land use transitions in the PYLB.

LUT	1990–2000		2000–2010		2010–2020	
	Area (ha)	Percent (%)	Area (ha)	Percent (%)	Area (ha)	Percent (%)
12	17,215	14.06	53,036	14.15	163,130	23.82
13	978	0.80	3886	1.04	14,442	2.11
14	12,568	10.27	22,440	5.99	17,015	2.48
15	11,984	9.79	70,069	18.70	93,059	13.59
16	0	0.00	55	0.01	40	0.01
21	12,182	9.95	66,486	17.74	166,271	24.28
23	12,257	10.01	10,628	2.84	62,716	9.16
24	2553	2.09	5067	1.35	10,927	1.60
25	3374	2.76	33,034	8.82	56,380	8.23
26	121	0.10	47	0.01	58	0.01
31	1086	0.89	11,291	3.01	13,432	1.96
32	35,162	28.72	43,712	11.67	23,469	3.43
34	403	0.33	1749	0.47	2055	0.30
35	392	0.32	4571	1.22	8185	1.20
36	3	0.00	8	0.00	23	0.00
41	10,156	8.30	30,303	8.09	13,336	1.95
42	622	0.51	4233	1.13	8312	1.21
43	717	0.59	877	0.23	1231	0.18
45	382	0.31	3554	0.95	3699	0.54
46	0	0.00	0	0.00	0	0.00
51	105	0.09	5958	1.59	20,423	2.98
52	28	0.02	1240	0.33	4271	0.62
53	4	0.00	122	0.03	828	0.12
54	7	0.01	1961	0.52	1284	0.19
56	0	0.00	1	0.00	4	0.00
61	0	0.00	68	0.02	34	0.00
62	125	0.10	220	0.06	61	0.01
63	0	0.00	8	0.00	19	0.00
64	0	0.00	14	0.00	2	0.00
65	0	0.00	83	0.02	76	0.01
Total	122,424	100.00	374,721	100.00	684,779	100.00

Note: LUT is land use transition. Codes 1 to 6 are farmland, forestland, grassland, wetland, built-up land, and unused land, respectively, and code 12 is farmland converted to forestland; other codes follow the same rule.

3.3. Temporal Changes in Carbon Storage

The carbon storage in the basin was mainly in forestland and farmland, which occupied 65.74% and 23.85% in 2020, respectively (Table 4). Wetland, grassland, and built-up land occupied 5.37%, 3.90%, and 1.14%, respectively. The four carbon pools contributed differently to total carbon storage. The SOC was the largest carbon pool, which accounted for more than 72%, followed by AGC (about 19%). The proportion stored in BGC and DOC was relatively small. From 1990 to 2020, the total carbon storage decreased by 17.26 Tg (Table 5). The total carbon storage experienced an accelerating decreasing trend in the basin. Specifically, the total carbon storage decreased by 0.38 Tg, 6.72 Tg, and 10.16 Tg during 1990–2000, 2000–2010, and 2010–2020, respectively. With the exception of AGC, which increased by 0.17 Tg from 1990 to 2000, the four carbon pools all decreased during the past three decades in the study area.

Table 4. Changes in carbon storage of each land use type in the PYLB (unit: Tg).

Year	Land Use Type						Total
	Farmland	Forest	Grassland	Wetland	Built-Up Land	Unused Land	
1990	465.57	1256.59	77.67	101.58	10.70	0.10	1912.22
2000	463.53	1259.41	75.31	102.09	11.39	0.10	1911.83
2010	459.77	1257.81	70.61	101.01	15.83	0.09	1905.11
2020	451.88	1245.74	73.90	101.67	21.68	0.09	1894.95

Table 5. Changes in carbon storage of four carbon pools in the PYLB (unit: Tg).

Carbon Pool	Carbon Storage				Carbon Storage Change			
	1990	2000	2010	2020	1990–2000	2000–2010	2010–2020	1990–2020
AGC	364.06	364.23	363.43	361.04	−0.17	−0.80	−2.39	−3.01
BGC	127.82	127.49	126.38	125.80	−0.33	−1.12	−0.58	−2.02
DOC	38.83	38.81	38.58	38.27	−0.02	−0.23	−0.31	−0.56
SOC	1381.50	1381.29	1376.73	1369.84	−0.21	−4.57	−6.88	−11.66
Total	1912.22	1911.83	1905.11	1894.95	−0.38	−6.72	−10.16	−17.26

Note: AGC—Aboveground carbon. BGC—Belowground carbon. SOC—Soil organic carbon. DOC—Dead organic matter carbon.

3.4. Hotspots and Cold Spots of Changes in Carbon Storage

Hotspot analysis was conducted to analyze the spatial change in carbon storage (Figure 5). From 1990 to 2000, the hotspots of carbon storage change were mainly scattered across Shangrao, Jian, Pingxiang, and the southwest of Yichun. From 2000 to 2010, the area of hotspots of carbon storage change was less than in the previous period, and was mainly scattered throughout the south of Fuzhou, northeast of Nanchang, northwest of Jiujiang, and Guidong county of Hunan Province. From 2010 to 2020, the only hotspot of carbon storage change occurred in the southeast of Jiujiang. The cold spots of carbon storage change were mainly concentrated in urban regions and their surroundings during the three periods.

3.5. Contributions of LUTs to Change in Carbon Storage

Contributions of various LUTs to carbon storage change were analyzed (Table 6). From 1990 to 2020, the carbon storage gain induced by LUTs was 8,891,560 Mg, in which the contributions of LUTs 12, 32, 14, and 51 were 36.87%, 22.58%, 15.89%, and 13.01%, respectively. Carbon loss resulting from LUTs was 26,154,446 Mg, in which the contributions of LUTs 15, 25, 21, and 41 were 39.94%, 28.06%, 13.25%, and 5.65%, respectively. Specifically, from 1990 to 2000, carbon gain resulting from LUTs was 1,589,292 Mg, in which the contributions of LUTs 32, 14, and 12 were 48.23%, 27.19%, and 19.50%, respectively. The carbon loss was 1,972,593 Mg, and LUTs 15, 41, 25, 23, and 21 contributed 38.18%, 17.71%, 13.83%, 13.55%, and 11.12%, respectively. From 2000 to 2010, the carbon gain was 3,567,010 Mg, in which LUTs 12, 32, 14, and 51 induced 26.76%, 26.71%, 21.63%, and 10.50%, respectively. Meanwhile, the carbon loss was 10,284,938 Mg, in which LUTs 15, 25, 21, and 41 contributed 42.81%, 25.97%, 11.64%, and 10.13%, respectively. From 2010 to 2020, the carbon gain induced by LUTs was 6,151,937 Mg, in which the contributions of LUTs 12, 51, 14, and 32 were 47.73%, 20.86%, 9.51%, and 8.32%, respectively. In contrast, the carbon loss caused by LUTs was 16,313,595 Mg, in which LUTs 15, 25, 21, and 23 contributed 35.85%, 27.94%, 18.35%, and 8.38%, respectively.

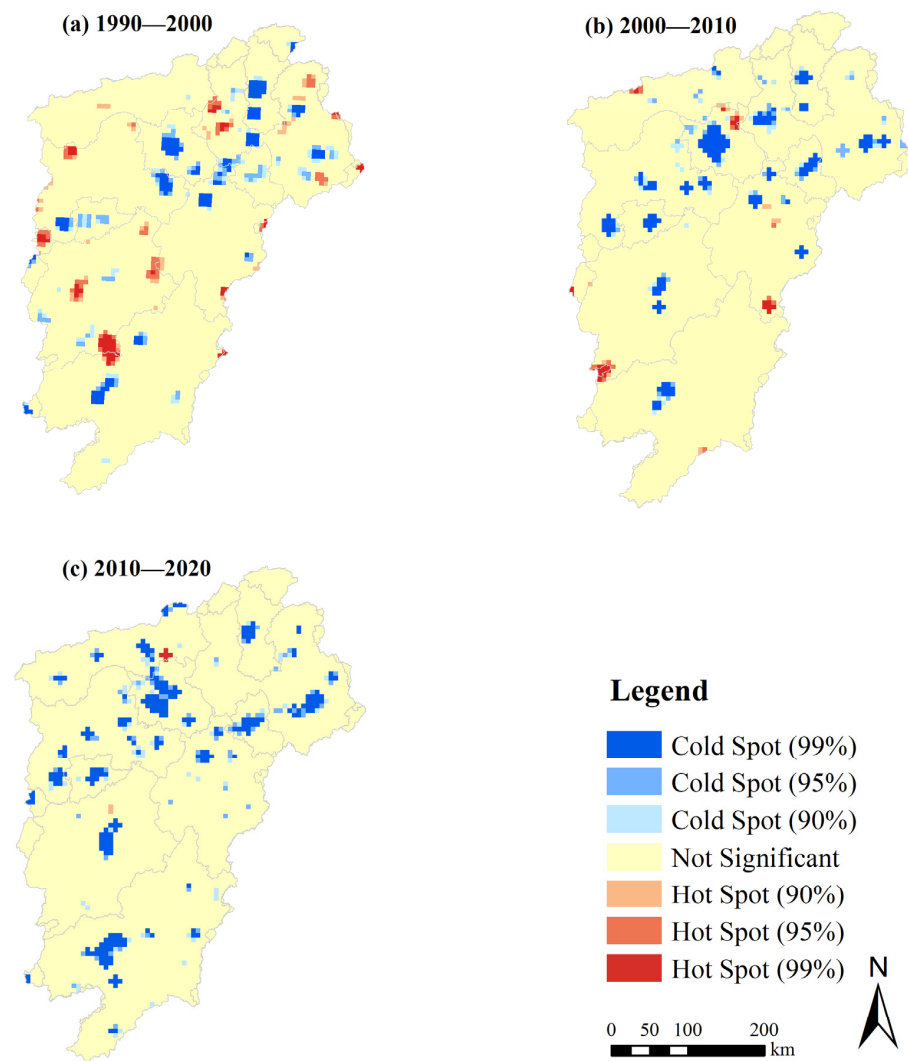


Figure 5. Spatial distribution of hotspots and cold spots of changes in carbon storage in the PYLB.

Table 6. Contribution of LUTs to carbon storage change in the PYLB.

Status	LUT	1990–2000		2000–2010		2010–2020		1990–2020	
		CS Change (Mg)	Percent (%)						
CS gain	12	309,864	19.50	954,655	26.76	2,936,346	47.73	3,277,984	36.87
	14	432,197	27.19	771,704	21.63	585,157	9.51	1,412,761	15.89
	24	41,840	2.63	83,050	2.33	179,087	2.91	239,727	2.70
	31	4127	0.26	42,906	1.20	51,040	0.83	83,381	0.94
	32	766,540	48.23	952,920	26.71	511,623	8.32	2,007,448	22.58
	34	15,398	0.97	66,783	1.87	78,479	1.28	140,333	1.58
	51	6600	0.42	374,384	10.50	1,283,352	20.86	1,156,847	13.01
	52	2234	0.14	100,229	2.81	345,264	5.61	273,155	3.07
	53	234	0.01	7195	0.20	48,864	0.79	25,112	0.28
	54	665	0.04	190,634	5.34	124,820	2.03	238,763	2.69
	56	0	0.00	3	0.00	16	0.00	16	0.00
	61	11	0.00	3995	0.11	2000	0.03	5469	0.06
	62	9569	0.60	16,825	0.47	4640	0.08	28,011	0.32
	63	15	0.00	458	0.01	1058	0.02	1147	0.01
	64	0	0.00	1271	0.04	192	0.00	1404	0.02
		Total	1,589,292	100.00	3,567,010	100.00	6,151,937	100.00	8,891,560

Table 6. Cont.

Status	LUT	1990–2000		2000–2010		2010–2020		1990–2020	
		CS Change (Mg)	Percent (%)						
CS loss	13	−3717	0.19	−14,768	0.14	−54,881	0.34	−57,847	0.22
	15	−753,066	38.18	−4,403,162	42.81	−5,847,800	35.85	−10,445,028	39.94
	16	−21	0.00	−3195	0.03	−2353	0.01	−4885	0.02
	21	−219,280	11.12	−1,196,739	11.64	−2,992,871	18.35	−3,464,683	13.25
	23	−267,199	13.55	−231,693	2.25	−1,367,202	8.38	−1,667,098	6.37
	25	−272,784	13.83	−2,670,502	25.97	−4,557,792	27.94	−7,338,527	28.06
	26	−9238	0.47	−3594	0.03	−4426	0.03	−13,933	0.05
	35	−23,141	1.17	−269,888	2.62	−483,213	2.96	−782,560	2.99
	36	−143	0.01	−413	0.00	−1240	0.01	−1413	0.01
	41	−349,257	17.71	−1,042,129	10.13	−458,620	2.81	−1,478,709	5.65
	42	−10,197	0.52	−69,374	0.67	−136,231	0.84	−153,030	0.59
	43	−27,377	1.39	−33,505	0.33	−47,016	0.29	−76,960	0.29
	45	−37,173	1.88	−345,574	3.36	−359,610	2.20	−669,105	2.56
	46	0	0.00	−42	0.00	−8	0.00	−8	0.00
	65	0	0.00	−361	0.00	−330	0.00	−661	0.00
	Total		−1,972,593	100.00	−10,284,938	100.00	−16,313,595	100.00	−26,154,446

4. Discussion

4.1. Impact of Land Use Change on Carbon Storage

Land use change can significantly affect carbon storage [49]. In this study, the results revealed that the PYLB has experienced dramatic land use change, which resulted in a net loss of 17.26 Tg in carbon storage from 1990 to 2020. Urbanization can accelerate built-up land expansion, which eliminated a large amount of farmland, forestland, and wetland and induced significant ecosystem degradation [9,50]. Since the strategies of the Central Region Rise and the Yangtze River Economic Belt, the PYLB has experienced rapid economic development and urbanization [35,51], which has been characterized by remarkable built-up land expansion and has led to considerable carbon loss. In this study, LUTs resulted in 26.15 Tg of carbon loss from 1990 to 2020. Conversion from farmland and forestland to built-up land resulted in 10.45 Tg and 7.34 Tg of carbon loss, contributing 39.94% and 28.06% of carbon loss during the study period, respectively. This indicated that built-up land expansion was the dominant contributor to carbon loss in the PYLB. This was consistent with previous studies [13,24]. In this study, built-up land expanded by 159.89 km², 1020.31 km², and 1345.89 km² during 1990–2000, 2000–2010, and 2010–2020, respectively, indicating that the PYLB experienced an accelerating urbanization process. Urbanization is expected to put more pressure on ecosystems in the future, leading to more carbon loss. Therefore, attention should be paid to the carbon loss resulting from built-up land expansion.

Previous studies indicated that farmland reclamation mainly occupied forests and wetlands, which resulted in considerable carbon loss [29,52]. Farmland expansion was also an important contributor to carbon loss in the PYLB. Conversion from forestland and wetland to farmland caused 3.46 Tg and 1.48 Tg of carbon loss, accounting for 13.25% and 5.65% of the total carbon loss from 1990 to 2020, respectively. This should be mainly ascribed to the “Requisition-compensation balance of farmland” (RCBF) policy. During past decades, China experienced rapid urbanization, which induced a large amount of farmland encroachment by built-up land and threatened food security [53,54]. Therefore, China launched the RCBF policy, to ensure food security, in 1997. This policy stated that the occupied farmland must be compensated by new farmland of the same quantity and quality [55]. However, it facilitated conversions from forestland, grassland, and wetland to farmland and induced ecosystem degradation. For example, Tang et al. [29] reported that farmland expansion resulted in 1.76 Tg of carbon loss in Hubei province from 2000 to 2010, which was mainly due to the RCBF policy. Chen et al. [35] revealed that the occupation

of forestland by farmland was the dominant contributor to the decrease in ecosystem service value in the middle reaches of the Yangtze River Economic Belt from 1995 to 2015. Moreover, built-up land expansion mainly occupied plains farmland, while the newly added farmland was mainly sloping and terrace farmland. As reported by Chen et al. [56], the slope of unstable farmland increased by 0.48° in China from 1990 to 2019. The PYLB is a subtropical basin with high rainfall erosivity, and the new farmland mostly occurred on steep slopes, which not only resulted in carbon loss but also severe soil erosion, thereby threatening local ecological security.

During past decades, to mitigate ecosystem degradation, the Chinese government has implemented multiple ecological restoration programs, such as the Grain for Green program and the natural forest conservation program [30]. These programs have significantly improved ecosystem services [49,57,58]. In PYLB, the Mountain–River–Lake Program has also been implemented to systematically control soil erosion. These ecological restoration programs have promoted forestland expansion, which was the dominant contributor to carbon gain in the PYLB during the past three decades. Specifically, conversion from farmland to forestland resulted in 3.28 Tg of carbon gain, accounting for 36.87% of carbon gain from 1990 to 2020. This is likely mainly due to the Grain for Green program, which aimed to return farmland on the steep hills to forestland. Meanwhile, conversion from grassland to forestland has resulted in 2.01 Tg of carbon gain, responsible for 22.58% of carbon gain, which indicates that the ecological restoration programs have made great achievements in the PYLB. This is in agreement with previous studies [18,23,25,26]. Moreover, we found that the main measures of ecological restoration programs in the PYLB varied over different periods. From 1990 to 2000, conversion from grassland to forestland produced 48.23% of carbon gain, while conversion from farmland to forestland produced 19.50% of carbon gain, which means that grassland afforestation was the main measure. From 2000 to 2010, conversion from farmland and grassland contributed 26.76% and 26.71% of carbon gain, implying that both returning farmland to forest and grassland afforestation were important measures. From 2010 to 2020, the contribution of the transition from farmland to forestland was much higher than that from grassland to forestland (47.73% vs. 8.32%) to carbon gain, which indicates that returning farmland to forestland became the main measure. A similar phenomenon was observed in Guizhou Province, China [59].

Wetlands cover about 6% of the terrestrial surface and provide important ecosystem services to people [60]. However, more than 50% of global wetlands have been lost during the last century, and farmland encroachment is the dominant driver [52,61–63]. In this study, conversion from farmland to wetland produced 15.89% of carbon gain, which can be ascribed to the Grain for Blue Program, which aims to protect wetlands by returning farmland to wetlands or water areas [64]. Moreover, the contribution of conversion from wetland to farmland to carbon loss decreased from 17.71% during 1990–2000 to 2.81% during 2010–2020, indicating that wetland protection measures have made great achievements. In general, built-up land is inconvertible to other land use types. However, this study found that the conversion from built-up land to farmland contributed 13.01% of carbon gain. This could be mainly due to the RCBF policy and the urban built-up land increase vs. rural built-up land decrease policy [35,55]. Gao et al. [65] reported that 13,938 km² of built-up land has been converted into farmland, which has led to an increase of 2.85 Tg in vegetation carbon in China from 2010 to 2015.

4.2. Policy Implication

Understanding the relationship between land use change and carbon storage can contribute to climate change mitigation and sustainable development [5]. However, most previous studies only estimate the carbon storage change resulting from land use change, while failing to reflect the internal gain and loss of carbon storage during the study period. To fill this gap, this study used the InVEST model and Geo-information Tupu method to quantitatively evaluate the contribution of various LUTs to carbon storage change, which can provide more detailed information for formulation and optimization of land use

policies to achieve carbon neutrality and sustainable development in the PYLB. Moreover, it can also be applied in other regions. In this study, expansions of forestland and wetland have resulted in considerable carbon gain, which indicates that ecological restoration programs have made great achievements in the basin. However, built-up expansion has resulted in considerable carbon loss during the study period. Meanwhile, the urbanization process is accelerating in the basin, which is expected to result more carbon loss in the future. Therefore, the loss in ecosystem services, including carbon storage, caused by urban expansion should be taken into consideration in urban planning. This is vital to realize carbon neutrality and sustainable development. Since 2022, China's population has begun to decline, which undoubtedly means lower food demand in the future. In addition, with the progress of modern agricultural technology, the yield per unit area will increase, which will further weaken the food crisis. However, the RCBF policy has promoted the conversion of ecological land to farmland in the PYLB. This partly offset the benefit of ecological restoration programs and resulted in ecosystem degradation. Therefore, we recommend that the RCBF policy be reconsidered [29,66,67].

4.3. Uncertainties and Limitations

The InVEST model estimates carbon storage based on carbon density and land use data. Firstly, the carbon density data used in this study were derived from previous research, not through field measurement. In future research, performing field sampling and surveying will improve the accuracy of carbon storage assessment. Secondly, the InVEST model assumes that the carbon density of each land use type remains unchanged, which brings uncertainties. However, the ecosystem usually experiences natural succession, and the carbon density tends to increase. In addition, human activities also significantly affect regional carbon density. Therefore, long-term continuous measurement of carbon density in the study area will reduce the uncertainty in the results. Thirdly, the InVEST model mainly focuses on the difference in carbon density between land use types, while ignoring the heterogeneity of the individual land use type. Taking forestland, for example, the conversion from broadleaf forest to shrub will undoubtedly change carbon density. In this study, the land use data with a spatial resolution of 30 m were obtained from the Resource and Environment Science Data Center of the Chinese Academy of Sciences (<https://www.resdc.cn/>, accessed on 21 May 2022), which has an accuracy higher than 92.90% [44]. However, it only contains six primary categories. Estimating carbon storage with more detailed land use data, such as data based on vegetation types, will improve the accuracy of the results, which should be a future direction.

5. Conclusions

This study quantified the contributions of various LUTs to carbon storage change in the PYLB based on the InVEST model and Geo-information Tupu method. The main conclusions are as follows: (1) The area of built-up land increased continuously, while the area of farmland continued to decrease from 1990 to 2020; (2) The PYLB has experienced a net decrease of 17.26 Tg in carbon storage during the past three decades; (3) The transition of 'farmland to forestland' contributed the most to carbon gain, with a proportion of 36.87%, followed by 'grassland to forestland' (22.58%), and 'farmland to water' (15.89%). In contrast, the transitions of 'farmland to built-up land', 'forestland to built-up land', and 'forestland to grassland' contributed the most to carbon loss, with proportions of 39.94%, 28.06%, and 13.25%, respectively. The results of this study can provide references for achieving carbon neutrality and sustainable development in the PYLB.

Author Contributions: Conceptualization, Y.W.; Methodology, Y.W.; Investigation, Y.W.; Writing—original draft, Y.W.; Writing—review & editing, Z.Z. and X.C.; Visualization, Y.W.; Supervision, Z.Z. and X.C.; Project administration, Z.Z.; Funding acquisition, Z.Z. All authors have read and agreed to the published version of the manuscript.

Funding: This paper was financially supported by the National Natural Science Foundation of China (Grant No. 41971025), Research Funding of China Three Gorges Corporation [grant number 202003251], the National Key Research and Development Project of China (Grant No. 2019YFC0409004), and the Postgraduate Research & Practice Innovation Program of Jiangsu Province (No. KYCX22_0634).

Data Availability Statement: The data that support the findings of this study are available from the corresponding author upon reasonable request.

Conflicts of Interest: The authors declare no conflict of interest.

References

1. Wang, Z.; Li, X.; Mao, Y.; Li, L.; Wang, X.; Lin, Q. Dynamic simulation of land use change and assessment of carbon storage based on climate change scenarios at the city level: A case study of Bortala, China. *Ecol. Indic.* **2022**, *134*, 108499. [\[CrossRef\]](#)
2. Cramer, W.; Guiot, J.; Fader, M.; Garrabou, J.; Gattuso, J.-P.; Iglesias, A.; Lange, M.A.; Lionello, P.; Llasat, M.C.; Paz, S.; et al. Climate change and interconnected risks to sustainable development in the Mediterranean. *Nat. Clim. Chang.* **2018**, *8*, 972–980. [\[CrossRef\]](#)
3. Tokarska, K.B.; Gillett, N.P. Cumulative carbon emissions budgets consistent with 1.5 °C global warming. *Nat. Clim. Chang.* **2018**, *8*, 296–299. [\[CrossRef\]](#)
4. Mendoza-Ponce, A.; Corona-Núñez, R.; Kraxner, F.; Leduc, S.; Patrizio, P. Identifying effects of land use cover changes and climate change on terrestrial ecosystems and carbon stocks in Mexico. *Glob. Environ. Chang.* **2018**, *53*, 12–23. [\[CrossRef\]](#)
5. Aneseyee, A.B.; Soromessa, T.; Elias, E.; Noszczyk, T.; Hernik, J.; Benti, N.E. Expressing carbon storage in economic terms: The case of the upper Omo Gibe Basin in Ethiopia. *Sci. Total Environ.* **2022**, *808*, 152166. [\[CrossRef\]](#)
6. Babbar, D.; Areendran, G.; Sahana, M.; Sarma, K.; Raj, K.; Sivadas, A. Assessment and prediction of carbon sequestration using Markov chain and InVEST model in Sariska Tiger Reserve, India. *J. Clean. Prod.* **2021**, *278*, 123333. [\[CrossRef\]](#)
7. Dybala, K.E.; Steger, K.; Walsh, R.G.; Smart, D.R.; Gardali, T.; Seavy, N.E.; Macinnis-Ng, C. Optimizing carbon storage and biodiversity co-benefits in reforested riparian zones. *J. Appl. Ecol.* **2018**, *56*, 343–353. [\[CrossRef\]](#)
8. Tian, L.; Tao, Y.; Fu, W.; Li, T.; Ren, F.; Li, M. Dynamic Simulation of Land Use/Cover Change and Assessment of Forest Ecosystem Carbon Storage under Climate Change Scenarios in Guangdong Province, China. *Remote Sens.* **2022**, *14*, 2330. [\[CrossRef\]](#)
9. Xiang, S.; Wang, Y.; Deng, H.; Yang, C.; Wang, Z.; Gao, M. Response and multi-scenario prediction of carbon storage to land use/cover change in the main urban area of Chongqing, China. *Ecol. Indic.* **2022**, *142*, 109205. [\[CrossRef\]](#)
10. Yang, H.; Huang, J.; Liu, D. Linking climate change and socioeconomic development to urban land use simulation: Analysis of their concurrent effects on carbon storage. *Appl. Geogr.* **2020**, *115*, 102135. [\[CrossRef\]](#)
11. Rajbanshi, J.; Das, S. Changes in carbon stocks and its economic valuation under a changing land use pattern—A multitemporal study in Konar catchment, India. *Land Degrad. Dev.* **2021**, *32*, 3573–3587. [\[CrossRef\]](#)
12. Gao, J.; Wang, L. Embedding spatiotemporal changes in carbon storage into urban agglomeration ecosystem management—A case study of the Yangtze River Delta, China. *J. Clean. Prod.* **2019**, *237*, 117764. [\[CrossRef\]](#)
13. He, C.; Zhang, D.; Huang, Q.; Zhao, Y. Assessing the potential impacts of urban expansion on regional carbon storage by linking the LUSD-urban and InVEST models. *Environ. Model. Softw.* **2016**, *75*, 44–58. [\[CrossRef\]](#)
14. Han, J.; Hu, Z.; Mao, Z.; Li, G.; Liu, S.; Yuan, D.; Guo, J. How to Account for Changes in Carbon Storage from Coal Mining and Reclamation in Eastern China? Taking Yanzhou Coalfield as an Example to Simulate and Estimate. *Remote Sens.* **2022**, *14*, 2014. [\[CrossRef\]](#)
15. Hutyra, L.R.; Yoon, B.; Hepinstall-Cymerman, J.; Alberti, M. Carbon consequences of land cover change and expansion of urban lands: A case study in the Seattle metropolitan region. *Landsc. Urban Plan.* **2011**, *103*, 83–93. [\[CrossRef\]](#)
16. Raciti, S.M.; Hutyra, L.R.; Newell, J.D. Mapping carbon storage in urban trees with multi-source remote sensing data: Relationships between biomass, land use, and demographics in Boston neighborhoods. *Sci. Total Environ.* **2014**, *500–501*, 72–83. [\[CrossRef\]](#)
17. Nelson, E.; Mendoza, G.; Regetz, J.; Polasky, S.; Tallis, H.; Cameron, D.; Chan, K.M.A.; Daily, G.C.; Goldstein, J.; Kareiva, P.M.; et al. Modeling multiple ecosystem services, biodiversity conservation, commodity production, and tradeoffs at landscape scales. *Front. Ecol. Environ.* **2009**, *7*, 4–11. [\[CrossRef\]](#)
18. Zhou, J.; Zhao, Y.; Huang, P.; Zhao, X.; Feng, W.; Li, Q.; Xue, D.; Dou, J.; Shi, W.; Wei, W.; et al. Impacts of ecological restoration projects on the ecosystem carbon storage of inland river basin in arid area, China. *Ecol. Indic.* **2020**, *118*, 106803. [\[CrossRef\]](#)
19. Zhao, M.; Yue, T.; Zhao, N.; Sun, X.; Zhang, X. Combining LPJ-GUESS and HASM to simulate the spatial distribution of forest vegetation carbon stock in China. *J. Geogr. Sci.* **2014**, *24*, 249–268. [\[CrossRef\]](#)
20. Parton, W.J.; Scurlock, J.M.O.; Ojima, D.S.; Gilmanov, T.G.; Scholes, R.J.; Schimel, D.S.; Kirchner, T.; Menaut, J.C.; Seastedt, T.; Moya, E.G.; et al. Observations and Modeling of Biomass and Soil Organic-Matter Dynamics for the Grassland Biome Worldwide. *Glob. Biogeochem. Cycles* **1993**, *7*, 785–809. [\[CrossRef\]](#)
21. Melillo, J.M.; Borchers, J.; Chaney, J.; Fisher, H.; Fox, S.; Haxeltine, A.; Janetos, A.; Kicklighter, D.W.; Kittel, T.G.F.; Mcguire, A.D.; et al. Vegetation Ecosystem Modeling and Analysis Project-Comparing Biogeography and Biogeochemistry Models in a Continental-Scale Study of Terrestrial Ecosystem Responses to Climate-Change and CO₂ Doubling. *Glob. Biogeochem. Cycles* **1995**, *9*, 407–437. [\[CrossRef\]](#)

22. Brilli, L.; Bechini, L.; Bindi, M.; Carozzi, M.; Cavalli, D.; Conant, R.; Dorich, C.D.; Doro, L.; Ehrhardt, F.; Farina, R.; et al. Review and analysis of strengths and weaknesses of agro-ecosystem models for simulating C and N fluxes. *Sci. Total Environ.* **2017**, *598*, 445–470. [[CrossRef](#)] [[PubMed](#)]
23. Liang, Y.; Hashimoto, S.; Liu, L. Integrated assessment of land-use/land-cover dynamics on carbon storage services in the Loess Plateau of China from 1995 to 2050. *Ecol. Indic.* **2021**, *120*, 106939. [[CrossRef](#)]
24. Jiang, W.; Deng, Y.; Tang, Z.; Lei, X.; Chen, Z. Modelling the potential impacts of urban ecosystem changes on carbon storage under different scenarios by linking the CLUE-S and the InVEST models. *Ecol. Model.* **2017**, *345*, 30–40. [[CrossRef](#)]
25. Zhao, M.; He, Z.; Du, J.; Chen, L.; Lin, P.; Fang, S. Assessing the effects of ecological engineering on carbon storage by linking the CA-Markov and InVEST models. *Ecol. Indic.* **2019**, *98*, 29–38. [[CrossRef](#)]
26. Hu, X.Q.; Li, Z.W.; Chen, J.; Nie, X.D.; Liu, J.Y.; Wang, L.X.; Ning, K. Carbon sequestration benefits of the grain for Green Program in the hilly red soil region of southern China. *Int. Soil Water Conserv. Res.* **2021**, *9*, 271–278. [[CrossRef](#)]
27. Wei, P.; Chen, S.; Wu, M.; Jia, Y.; Xu, H.; Liu, D. Increased Ecosystem Carbon Storage between 2001 and 2019 in the Northeastern Margin of the Qinghai-Tibet Plateau. *Remote Sens.* **2021**, *13*, 3986. [[CrossRef](#)]
28. Li, J.; Gong, J.; Guldmann, J.-M.; Li, S.; Zhu, J. Carbon Dynamics in the Northeastern Qinghai-Tibetan Plateau from 1990 to 2030 Using Landsat Land Use/Cover Change Data. *Remote Sens.* **2020**, *12*, 528. [[CrossRef](#)]
29. Tang, L.; Ke, X.; Zhou, T.; Zheng, W.; Wang, L. Impacts of cropland expansion on carbon storage: A case study in Hubei, China. *J. Environ. Manag.* **2020**, *265*, 110515. [[CrossRef](#)]
30. Ouyang, Z.; Zheng, H.; Xiao, Y.; Polasky, S.; Liu, J.; Xu, W.; Wang, Q.; Zhang, L.; Xiao, Y.; Rao, E.; et al. Improvements in ecosystem services from investments in natural capital. *Science* **2016**, *352*, 1455–1459. [[CrossRef](#)]
31. Zhu, G.; Qiu, D.; Zhang, Z.; Sang, L.; Liu, Y.; Wang, L.; Zhao, K.; Ma, H.; Xu, Y.; Wan, Q. Land-use changes lead to a decrease in carbon storage in arid region, China. *Ecol. Indic.* **2021**, *127*, 107770. [[CrossRef](#)]
32. Chu, X.; Zhan, J.; Li, Z.; Zhang, F.; Qi, W. Assessment on forest carbon sequestration in the Three-North Shelterbelt Program region, China. *J. Clean. Prod.* **2019**, *215*, 382–389. [[CrossRef](#)]
33. Ye, Q.; Tian, G.; Liu, G.; Ye, J.; Yao, X.; Liu, Q.; Lou, W.; Wu, S. Tupu methods of spatial-temporal pattern on land use change: A case study in the Yellow River Delta. *J. Geogr. Sci.* **2004**, *14*, 131–142. [[CrossRef](#)]
34. Lu, X.; Shi, Y.; Chen, C.; Yu, M. Monitoring cropland transition and its impact on ecosystem services value in developed regions of China: A case study of Jiangsu Province. *Land Use Policy* **2017**, *69*, 25–40. [[CrossRef](#)]
35. Chen, W.; Zhao, H.; Li, J.; Zhu, L.; Wang, Z.; Zeng, J. Land use transitions and the associated impacts on ecosystem services in the Middle Reaches of the Yangtze River Economic Belt in China based on the geo-informatic Tupu method. *Sci. Total Environ.* **2020**, *701*, 134690. [[CrossRef](#)] [[PubMed](#)]
36. Liang, X.; Jin, X.; Ren, J.; Gu, Z.; Zhou, Y. A research framework of land use transition in Suzhou City coupled with land use structure and landscape multifunctionality. *Sci. Total Environ.* **2020**, *737*, 139932. [[CrossRef](#)]
37. Song, Y.; Wang, M.; Sun, X.; Fan, Z. Quantitative assessment of the habitat quality dynamics in Yellow River Basin, China. *Environ. Monit. Assess.* **2021**, *193*, 614. [[CrossRef](#)]
38. Wang, Q.; Yang, K.; Li, L.; Zhu, Y. Assessing the Terrain Gradient Effect of Landscape Ecological Risk in the Dianchi Lake Basin of China Using Geo-Information Tupu Method. *Int. J. Environ. Res. Public Health* **2022**, *19*, 9634. [[CrossRef](#)]
39. Wang, Y.; Zhang, Z.; Chen, X. Quantifying Influences of Natural and Anthropogenic Factors on Vegetation Changes Based on Geodetector: A Case Study in the Poyang Lake Basin, China. *Remote Sens.* **2021**, *13*, 5081. [[CrossRef](#)]
40. Liu, F.-h.; Xu, C.-Y.; Yang, X.-x.; Ye, X.-c. Controls of Climate and Land-Use Change on Terrestrial Net Primary Productivity Variation in a Subtropical Humid Basin. *Remote Sens.* **2020**, *12*, 3525. [[CrossRef](#)]
41. Wang, R.; Peng, W.; Liu, X.; Jiang, C.; Wu, W.; Chen, X. Characteristics of Runoff Variations and Attribution Analysis in the Poyang Lake Basin over the Past 55 Years. *Sustainability* **2020**, *12*, 944. [[CrossRef](#)]
42. Getis, A.; Ord, J.K. The Analysis of Spatial Association by Use of Distance Statistics. *Geogr. Anal.* **1992**, *24*, 189–206. [[CrossRef](#)]
43. Liu, J.; Kuang, W.; Zhang, Z.; Xu, X.; Qin, Y.; Ning, J.; Zhou, W.; Zhang, S.; Li, R.; Yan, C.; et al. Spatiotemporal characteristics, patterns, and causes of land-use changes in China since the late 1980s. *J. Geogr. Sci.* **2014**, *24*, 195–210. [[CrossRef](#)]
44. Chuai, X.; Huang, X.; Lai, L.; Wang, W.; Peng, J.; Zhao, R. Land use structure optimization based on carbon storage in several regional terrestrial ecosystems across China. *Environ. Sci. Policy* **2013**, *25*, 50–61. [[CrossRef](#)]
45. Lai, L. Carbon Emission Effect of Land Use in China. Ph.D. Thesis, Nanjing University, Nanjing, China, 2010.
46. Liu, G.; Chen, L. Study on carbon storage in Honghu lake wetland. *J. Cent. South Univ. For. Technol.* **2013**, *33*, 103–107.
47. Xi, X.; Li, M.; Zhang, X.; Zhang, Y.; Zhang, D.; Zhang, J.; Dou, L.; Yang, Y. Research on soil organic carbon distribution and change trend in middle-east plain and its vicinity in China. *Earth Sci. Front.* **2013**, *20*, 154–165.
48. Ke, X.; Tang, L. Impact of cascading processes of urban expansion and cropland reclamation on the ecosystem of a carbon storage service in Hubei Province, China. *Acta Ecol. Sin.* **2019**, *39*, 672–683.
49. Lu, F.; Hu, H.; Sun, W.; Zhu, J.; Liu, G.; Zhou, W.; Zhang, Q.; Shi, P.; Liu, X.; Wu, X.; et al. Effects of national ecological restoration projects on carbon sequestration in China from 2001 to 2010. *Proc. Natl. Acad. Sci. USA* **2018**, *115*, 4039–4044. [[CrossRef](#)] [[PubMed](#)]
50. Tang, L.; Ke, X.; Zhou, Q.; Wang, L.; Koomen, E. Projecting future impacts of cropland reclamation policies on carbon storage. *Ecol. Indic.* **2020**, *119*, 106835. [[CrossRef](#)]
51. Xie, H.; He, Y.; Choi, Y.; Chen, Q.; Cheng, H. Warning of negative effects of land-use changes on ecological security based on GIS. *Sci. Total Environ.* **2020**, *704*, 135427. [[CrossRef](#)]

52. Mao, D.; Luo, L.; Wang, Z.; Wilson, M.C.; Zeng, Y.; Wu, B.; Wu, J. Conversions between natural wetlands and farmland in China: A multiscale geospatial analysis. *Sci. Total Environ.* **2018**, *634*, 550–560. [[CrossRef](#)] [[PubMed](#)]
53. Jiang, L.; Deng, X.; Seto, K.C. Multi-level modeling of urban expansion and cultivated land conversion for urban hotspot counties in China. *Landsc. Urban Plan.* **2012**, *108*, 131–139. [[CrossRef](#)]
54. Chen, W.; Ye, X.; Li, J.; Fan, X.; Liu, Q.; Dong, W. Analyzing requisition–compensation balance of farmland policy in China through telecoupling: A case study in the middle reaches of Yangtze River Urban Agglomerations. *Land Use Policy* **2019**, *83*, 134–146. [[CrossRef](#)]
55. Shen, X.; Wang, L.; Wu, C.; Lv, T.; Lu, Z.; Luo, W.; Li, G. Local interests or centralized targets? How China’s local government implements the farmland policy of Requisition–Compensation Balance. *Land Use Policy* **2017**, *67*, 716–724. [[CrossRef](#)]
56. Chen, H.; Tan, Y.; Xiao, W.; Li, G.; Meng, F.; He, T.; Li, X. Urbanization in China drives farmland uphill under the constraint of the requisition–compensation balance. *Sci. Total Environ.* **2022**, *831*, 154895. [[CrossRef](#)]
57. Tong, X.; Brandt, M.; Yue, Y.; Horion, S.; Wang, K.; Keersmaecker, W.D.; Tian, F.; Schurgers, G.; Xiao, X.; Luo, Y.; et al. Increased vegetation growth and carbon stock in China karst via ecological engineering. *Nat. Sustain.* **2018**, *1*, 44–50. [[CrossRef](#)]
58. Chen, C.; Park, T.; Wang, X.; Piao, S.; Xu, B.; Chaturvedi, R.K.; Fuchs, R.; Brovkin, V.; Ciais, P.; Fensholt, R.; et al. China and India lead in greening of the world through land-use management. *Nat. Sustain.* **2019**, *2*, 122–129. [[CrossRef](#)]
59. Wang, Y.; Zhang, Z.; Chen, X. Spatiotemporal change in ecosystem service value in response to land use change in Guizhou Province, southwest China. *Ecol. Indic.* **2022**, *144*, 109514. [[CrossRef](#)]
60. Zedler, J.B.; Kercher, S. Wetland Resources: Status, Trends, Ecosystem Services, and Restorability. *Annu. Rev. Environ. Resour.* **2005**, *30*, 39–74. [[CrossRef](#)]
61. Davidson, N.C. How much wetland has the world lost? Long-term and recent trends in global wetland area. *Mar. Freshw. Res.* **2014**, *65*, 934–941. [[CrossRef](#)]
62. Beuel, S.; Alvarez, M.; Amler, E.; Behn, K.; Kotze, D.; Kreye, C.; Leemhuis, C.; Wagner, K.; Willy, D.K.; Ziegler, S.; et al. A rapid assessment of anthropogenic disturbances in East African wetlands. *Ecol. Indic.* **2016**, *67*, 684–692. [[CrossRef](#)]
63. Fluet-Chouinard, E.; Stocker, B.D.; Zhang, Z.; Malhotra, A.; Melton, J.R.; Poulter, B.; Kaplan, J.O.; Goldewijk, K.K.; Siebert, S.; Minayeva, T.; et al. Extensive global wetland loss over the past three centuries. *Nature* **2023**, *614*, 281–286. [[CrossRef](#)] [[PubMed](#)]
64. Song, W.; Deng, X.; Liu, B.; Li, Z.; Jin, G. Impacts of Grain-for-Green and Grain-for-Blue Policies on Valued Ecosystem Services in Shandong Province, China. *Adv. Meteorol.* **2015**, *2015*, 213534. [[CrossRef](#)]
65. Gao, R.; Chuai, X.; Ge, J.; Wen, J.; Zhao, R.; Zuo, T. An integrated tele-coupling analysis for requisition–compensation balance and its influence on carbon storage in China. *Land Use Policy* **2022**, *116*, 106057. [[CrossRef](#)]
66. Liu, X.; Zhao, C.; Song, W. Review of the evolution of cultivated land protection policies in the period following China’s reform and liberalization. *Land Use Policy* **2017**, *67*, 660–669. [[CrossRef](#)]
67. Wu, Y.; Shan, L.; Guo, Z.; Peng, Y. Cultivated land protection policies in China facing 2030: Dynamic balance system versus basic farmland zoning. *Habitat Int.* **2017**, *69*, 126–138. [[CrossRef](#)]

Disclaimer/Publisher’s Note: The statements, opinions and data contained in all publications are solely those of the individual author(s) and contributor(s) and not of MDPI and/or the editor(s). MDPI and/or the editor(s) disclaim responsibility for any injury to people or property resulting from any ideas, methods, instructions or products referred to in the content.